

Landauer's blow-torch effect in systems with entropic potential

Moupriya Das and Deb Shankar Ray*

Indian Association for the Cultivation of Science, Jadavpur, Kolkata-700032, India

(Received 17 June 2015; revised manuscript received 9 September 2015; published 23 November 2015)

We consider local heating of a part of a two-dimensional bilobal enclosure of a varying cross section confining a system of overdamped Brownian particles. Since varying cross section in higher dimension results in an entropic potential in lower dimension, local heating alters the relative stability of the entropic states. We show that this blow-torch effect modifies the entropic potential in a significant way so that the resultant effective entropic potential carries both the features of variation of width of the confinement and variation of temperature along the direction of transport. The reduced probability distribution along the direction of transport calculated by full numerical simulations in two dimensions agrees well with our analytical findings. The extent of population transfer in the steady state quantified in terms of the integrated probability of residence of the particles in either of the two lobes exhibits interesting variation with the mean position of the heated region. Our study reveals that heating around two particular zones of a given lobe maximizes population transfer to the other.

DOI: [10.1103/PhysRevE.92.052133](https://doi.org/10.1103/PhysRevE.92.052133)

PACS number(s): 05.40.Jc, 05.10.Gg

I. INTRODUCTION

An interesting class of problems was introduced by Landauer [1–5] where the steady state probability distribution depends on the details of the noise processes associated with the path which connects the states of local stability. For example, if some portion of a double-well potential near the barrier maximum is heated locally, the relative population of the two wells in the steady state differs from that of the equilibrium state value for the original system [1,2]. A related issue concerns the passage of Brownian particles through a very thin tube of a uniform cross section having spatially varying temperature [3]. The particles acquire the temperature of the wall through the collisions with it. The spatial variation of the temperature is such that the length of the tube having a certain temperature is long enough to allow the particles to come to thermal equilibrium with the local tube temperature. As expected, the particles accumulate in the colder regions where they move slowly, giving rise to peaks in the probability distribution curve at the positions of lower temperatures. The interesting point to note here is that the distribution function is actually flat for the original system. In spite of the absence of the states of local stability in the deterministic dynamics or devoid of the multiplicative nature of the noise present in the system, the system generates some states of local stability depending on the details of the fluctuation associated with the process. These effects are popularly known as Landauer's blow-torch effect [6–8].

In this paper, we focus our attention on Landauer's blow-torch effect on systems having varying cross-sectional width [9–13]. Specifically, our aim is to explore the influence of the confining geometry on population transfer through local heating of some parts of the system. The motivation lies on the following consideration. It is well known that when a Brownian particle moves through a tube or channel having varying cross section, the geometrical confinement in higher dimension gives rise to an effective entropic potential in reduced dimension [10–64]. The entropic transport occurring in systems with

varying geometry has attracted wide attention in recent years in the context of stochastic resonance [17,18], resonant activation [19], ratchets and molecular motors [20,25–27], particle separation mechanism through entropic splitting [40,53], entropic rectification [47,51], entropic Brownian pump [52], hysteresis [61,62], geometry-controlled kinetics [58,59], stochastic localization [24], construction of logic gates [63], entropic memory erasure [64], and also in the process of ion transport through phospholipid membranes, biological channels [30,31], artificial ion pumps [32–34], translocation of polymers and polynucleotides through nanopores [35], etc. While entropic transport processes as mentioned here take place at a constant temperature, spatial variation of temperature may occur naturally in some physical situations where the different parts of the system are kept in contact with different thermal baths. It is expected that this spatial inhomogeneity of temperature can significantly alter the relative stability of the entropic states and thereby influence the population transfer between them. In what follows, we show that the entropic potential is profoundly modified due to spatially varying temperature. The resultant effective potential captures the interference of two entropic effects, one due to geometrical confinement and the other due to the local heating that causes alteration of relative stability of the two states. Our analysis is based on consideration of an ensemble of overdamped Brownian particle confined in a two-dimensional bilobal enclosure. At a constant temperature, both the lobes get equally occupied. When some part of the system is kept at a higher temperature, the occupancy of the lobes differs from each other, leading to a splitting in the steady state population density for the two lobes. This is calculated in terms of the integrated probability of residence of the particles in either of the two lobes. The occupancy of the entropic steady states depends on the details of the kinetics of the different parts of the system [1]. The dependence of the population transfer on the position of the heated zone of the system is subjected to full numerical simulations in two dimensions. Our study reveals an interesting bimodal variation of the extent of population transfer as an entropic effect against the mean position of the heated zone, implying that the population transfer is most effective when two particular portions of a given lobe are

*pcdsr@iacs.res.in

heated separately. The modification of the entropic potential due to temperature variation is manifested in the numerically simulated reduced probability distribution curve which is obtained from the exact Brownian dynamics simulation of the two-dimensional system subjected to appropriate boundary condition representing the confining effect of the system. As expected, the effective population transfer depends on the difference in temperature of the baths and on the range of the system heated.

The paper is organized as follows. In Sec. II, we describe the system and the motion of an overdamped Brownian particle confined in the two-dimensional bilobal enclosure and in contact with two different thermal baths. The dynamics of the particle subjected to this variation of temperature is evaluated in terms of the Fick-Jacobs equation in the reduced dimension and the effective entropic potential is calculated. The numerical results based on simulation of exact Brownian dynamics in two dimensions have been presented and discussed in Sec. III. The paper is concluded in Sec. IV.

II. STOCHASTIC DYNAMICS IN CONFINED GEOMETRY WITH NONUNIFORM TEMPERATURE

A. Model

We consider an overdamped Brownian particle confined in a two-dimensional bilobal enclosure as shown in Fig. 1(a). The temperature as well as the frictional coefficient are spatially nonuniform along the longitudinal direction, i.e., they are functions of \tilde{x} coordinate of space variables. \tilde{x} represents the conventional longitudinal direction. The tilde description has been used to indicate that this is a dimensional quantity. We will represent all the quantities having dimension with tilde notation. The two-dimensional Langevin equation for the Brownian particle can be written as follows:

$$\tilde{\gamma}(\tilde{x}) \frac{d\vec{r}}{d\tilde{t}} = -\tilde{G}\hat{e}_y + \sqrt{\tilde{\gamma}(\tilde{x})k_B\tilde{T}(\tilde{x})}\vec{\eta}(\tilde{t}). \quad (2.1)$$

Here, \vec{r} represents the position vector of the particle and \hat{e}_y is the unit vector along the \tilde{y} direction. $\tilde{\gamma}(\tilde{x})$ denotes the frictional coefficient of the system at a particular \tilde{x} coordinate and it remains the same for all values of \tilde{y} for the given \tilde{x} . Similarly, $\tilde{T}(\tilde{x})$ represents temperature at a particular position \tilde{x} in the longitudinal direction. k_B stands for the Boltzmann constant. \tilde{G} is a very weak constant bias acting along the transverse direction of the system. $\vec{\eta}(\tilde{t}) = [\tilde{\eta}_x(\tilde{t}), \tilde{\eta}_y(\tilde{t})]$ is a zero mean, Gaussian, white noise, i.e.,

$$\begin{aligned} \langle \vec{\eta}(\tilde{t}) \rangle &= 0, \\ \langle \tilde{\eta}_i(\tilde{t})\tilde{\eta}_j(\tilde{t}') \rangle &= 2\delta_{ij}\delta(\tilde{t} - \tilde{t}'), \end{aligned} \quad (2.2)$$

for $i, j = \tilde{x}, \tilde{y}$.

The prefactor of $\vec{\eta}(\tilde{t})$ in Eq. (2.1) suggests that $\vec{\eta}(\tilde{t})$ obeys the fluctuation-dissipation relation. The physical confinement can be imposed on the particle's motion by using reflecting boundary condition at the walls of the enclosure. The walls of the bilobal system, as shown in Fig. 1(a), can be described by the following equation:

$$\tilde{\omega}_l(\tilde{x}) = -\tilde{\omega}_u(\tilde{x}) = L_y(\tilde{x}/L_x)^4 - 2L_y(\tilde{x}/L_x)^2 - \tilde{c}/2, \quad (2.3)$$

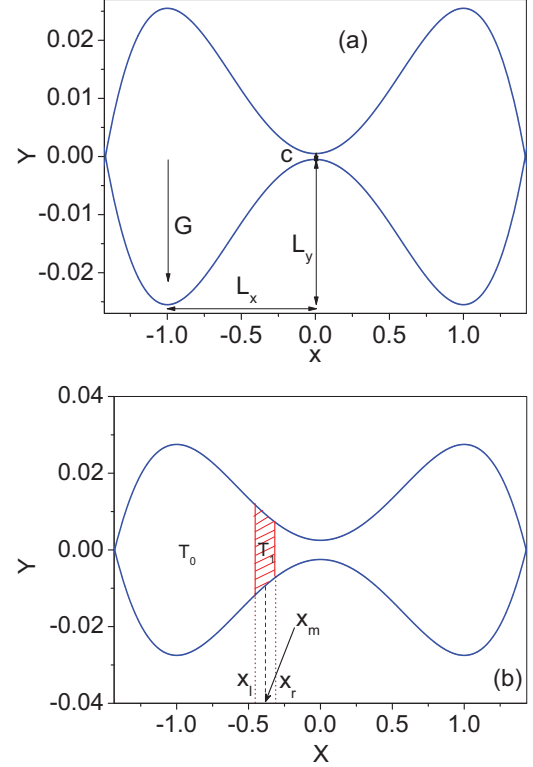


FIG. 1. (Color online) (a) The bilobal system with its geometrical parameters. (b) Schematic diagram of the system subjected to local heating. The shaded region corresponds to the heated zone. T_0 is the temperature of the low temperature bath and T_1 is the temperature of the high temperature bath. x_l and x_r stand for the position of the left and right boundaries of the heated zone, respectively, and x_m denotes their mean position.

where $\tilde{\omega}_l(\tilde{x})$ and $\tilde{\omega}_u(\tilde{x})$ represent the lower and the upper boundary functions, respectively, L_x denotes the distance between the middle point of the bottleneck and the position of the narrowing of the boundary functions, L_y corresponds to the remaining width at the bottleneck. Consequently, the local half-width of the structure is given by

$$\tilde{\omega}(\tilde{x}) = [\tilde{\omega}_u(\tilde{x}) - \tilde{\omega}_l(\tilde{x})]/2. \quad (2.4)$$

For further analysis, we use the dimensionless description [13–17,19–24] of the system with the help of the following scaled quantities. The length scales of the dynamics are made dimensionless with the characteristic length L_x . This leads to the scaled quantities $x = \tilde{x}/L_x$ and $y = \tilde{y}/L_x$, implying $c = \tilde{c}/L_x$. This ensures the scaled boundary functions and the local half-width represented as $\omega_l(x) = \tilde{\omega}_l(\tilde{x})/L_x = -\omega_u(x)$ and $\omega(x) = \tilde{\omega}(\tilde{x})/L_x$. The frictional coefficient $\tilde{\gamma}(\tilde{x})$ is made dimensionless with a reference damping constant γ_R at a reference temperature T_R and the dimensionless frictional coefficient is represented as $\gamma(x) = \tilde{\gamma}(\tilde{x})/\gamma_R$. The time \tilde{t} is scaled as $t = \tilde{t}/\tau$, where $\tau = \gamma_R L_x^2/k_B T_R$. τ is essentially twice the time required for a particle to traverse a distance L_x at temperature T_R in the medium with damping coefficient γ_R . The forces are scaled with the quantity $F_R = \gamma_R L_x/\tau$, i.e., $G = \tilde{G}\tau/\gamma_R L_x$. In dimensionless form, the Langevin equation

becomes

$$\frac{d\vec{r}}{dt} = -G(x)\hat{e}_y + \sqrt{D(x)}\vec{\eta}(t), \quad (2.5)$$

where $D(x)$ is the rescaled diffusion coefficient and is essentially the ratio of the scaled temperature $T(x) = \tilde{T}(\tilde{x})/T_R$ and the scaled damping constant $\gamma(x) = \tilde{\gamma}(\tilde{x})/\gamma_R$, i.e., $D(x)$ is given by $T(x)/\gamma(x)$. $\eta(t)$ is the properly scaled Langevin force which has been scaled by $\tau^{-1/2}$. A further point to note here is that \tilde{G} , which is considered as a constant bias initially, has become a function of x in the dimensionless description. We obtain this space dependence of the constant force in Eq. (2.5) since $G(x)$ is actually $G/\gamma(x)$. The spatial dependence of the damping constant induces space dependence into the force. However, the transverse force \tilde{G} has been introduced in the dynamics as a very weak bias and for numerical calculation it can be kept as zero as well. As a consequence, its variation does not alter the dynamics of the system from that with a purely constant bias in practice. So, we can keep it constant without losing any impact of the underlying physics of the problem. The two-dimensional Langevin equation [Eq. (2.5)] can be rewritten in two mutually perpendicular directions (x and y directions) as

$$\begin{aligned} \frac{dx}{dt} &= \sqrt{D(x)}\eta_x(t), \\ \frac{dy}{dt} &= -G + \sqrt{D(x)}\eta_y(t). \end{aligned} \quad (2.6)$$

Here, $\eta_x(t)$ and $\eta_y(t)$ are the components of the Langevin force $\eta(t)$ in x and y directions, respectively. The scaled boundary

function is given by

$$\omega(x) = [\omega_u(x) - \omega_l(x)]/2 = -ax^4 + bx^2 + c/2. \quad (2.7)$$

The aspect ratio has been defined as $a = L_y/L_x$ and $b = 2a$, i.e., a and b are appropriately scaled constants. This particular choice of physical confinement essentially captures analogous features of the classical setup of a quartic bistable potential which is considered as the standard model for the barrier crossing problems. The two lobes represent two entropic states of comparable stability [17]. This model has two large symmetric cavities which are connected by a small bottleneck. The consideration of spatial variation of temperature in this sort of arrangement might be of considerable importance because it has been reported [65] that within the human body, the temperature profile depends to a great extent on the geometry and the inhomogeneity of the body. Variable density and heat conductivity of various tissues and local heat production of different organs create a spatially varying temperature profile within the body. This in turn is supposed to affect the steady state density of various species in a given region as population transfer through biological channels would depend on the temperature profile of the system [1–3]. Our system is expected to serve as the minimal model to analyze mass transfer and steady state probability density of two states of comparable stability in this kind of scenario. To deal with the situation with higher complexity, a network of such systems may be arranged in a proper manner to represent the spatially distributed tissues and organs. Consideration of appropriate temperature profile in this setup would be helpful to explain the observed concentration of transported species.

B. Fokker-Planck equation in reduced dimension; temperature dependent effective entropic potential

Equation (2.6) can be alternatively written as follows:

$$\gamma(x)\frac{dx}{dt} = \sqrt{\gamma(x)T(x)}\eta_x(t), \quad \gamma(x)\frac{dy}{dt} = -G + \sqrt{\gamma(x)T(x)}\eta_y(t), \quad (2.8)$$

as G is a very weak force. The Fokker-Planck equation [66] corresponding to the Langevin dynamics [Eq. (2.8)] is given by

$$\frac{\partial P(x,y,t)}{\partial t} = \frac{\partial}{\partial x}\mu(x)\left\{\left[\frac{\partial}{\partial x}U(x,y)\right]P(x,y,t) + \frac{\partial}{\partial x}T(x)P(x,y,t)\right\} + \mu(x)\frac{\partial}{\partial y}\left[\frac{\partial}{\partial y}U(x,y)\right]P(x,y,t) + D(x)\frac{\partial^2}{\partial y^2}P(x,y,t), \quad (2.9)$$

where the potential function has the form $U(x,y) = Gy$. Here, $\mu(x) = 1/\gamma(x)$ which implies that $D(x) = \mu(x)T(x)$. We arrive at the above expression of the Fokker-Planck equation [Eq. (2.9)] since for the two-dimensional system, the scaled diffusion coefficient is considered to be nonuniform along the x direction; a given area within the x range between x_l to x_r is locally heated [Fig. 1(b)] and the temperature remains constant for all values of y at a particular x . As a consequence, the dynamics along the x direction gets modified due to the temperature gradient [7,67,68]. The significance of the above Fokker-Planck equation is noteworthy from a qualitative point of view. x and y are two independent degrees of freedom. For the one-dimensional case, space dependent diffusion coefficient gives rise to a diffusion equation [67] whose spatial derivative parts resemble the partial derivative parts along the x direction of Eq. (2.9). As the transverse direction is not subjected to spatial temperature variation, the partial derivatives along the y direction remain unaltered in the two-dimensional Fokker-Planck equation. Equation (2.9) can be rearranged and rewritten in the following alternative form:

$$\begin{aligned} \frac{\partial P(x,y,t)}{\partial t} &= \frac{\partial}{\partial x}D(x)\exp\left[-\frac{U(x,y)}{T(x)}\right]\frac{\partial}{\partial x}\exp\left[\frac{U(x,y)}{T(x)}\right]P(x,y,t) + \frac{\partial}{\partial x}[\mu(x)T'(x)]P(x,y,t) \\ &+ \frac{\partial}{\partial x}\left[\mu(x)\frac{T'(x)}{T(x)}U(x,y)\right]P(x,y,t) + D(x)\frac{\partial}{\partial y}\exp\left[-\frac{U(x,y)}{T(x)}\right]\frac{\partial}{\partial y}\exp\left[\frac{U(x,y)}{T(x)}\right]P(x,y,t). \end{aligned} \quad (2.10)$$

[Here, $T(x)$ is the dimensionless temperature. It may be considered to be equivalent to $k_B T$.]

The direction of interest in this problem is the longitudinal direction. Therefore, following Zwanzig [11], one can integrate the two-dimensional Fokker-Planck equation [Eq. (2.10)] over the transverse direction. This leads to the following equation:

$$\begin{aligned} \frac{\partial}{\partial t} \int dy P(x, y, t) &= \frac{\partial}{\partial x} D(x) \int dy \left\{ \exp\left[-\frac{U(x, y)}{T(x)}\right] \frac{\partial}{\partial x} \exp\left[\frac{U(x, y)}{T(x)}\right] P(x, y, t) \right\} \\ &+ \frac{\partial}{\partial x} \mu(x) T'(x) \int dy P(x, y, t) + \frac{\partial}{\partial x} \left[\mu(x) \frac{T'(x)}{T(x)} \right] \int dy U(x, y) P(x, y, t) \\ &+ D(x) \int dy \left\{ \frac{\partial}{\partial y} \exp\left[-\frac{U(x, y)}{T(x)}\right] \frac{\partial}{\partial y} \exp\left[\frac{U(x, y)}{T(x)}\right] P(x, y, t) \right\}. \end{aligned} \quad (2.11)$$

Here, $T'(x)$ corresponds to the derivative of $T(x)$ with respect to x . The last term in the parentheses can be integrated out to give the flux along the y direction which vanishes at the boundary. The above description of the dynamics of the Brownian particle can be further simplified by considering local equilibrium [11–17, 19–24, 36, 37, 41–45, 48–54] along the y direction. A considerable amount of work has been done on the modification and checking of validity of the reduction scheme of the two-dimensional description of the dynamics along the direction of transport in several contexts [36, 37, 41–45, 48–54]. The width of the two-dimensional system is very small compared to its length. Besides, the temperature is nonuniform along the x direction only and fixed over the entire y range for a particular value of x . Consequently, it is justified to assume that the motion along the y direction settles down much faster compared to that in the x direction. The description of the dynamics in the reduced dimension can be achieved by defining a local concentration $C(x, t)$ along the x direction which is obtained by integrating $P(x, y, t)$ over y [i.e., $C(x, t) = \int dy P(x, y, t)$] and an x -dependent effective potential $A(x)$ as $e^{-A(x)/T(x)} = \int dy e^{-U(x, y)/T(x)}$. This assumption leads to the following expression of a conditional local equilibrium probability density of y at a given x : $\rho(y; x) = e^{-U(x, y)/T(x)} / e^{-A(x)/T(x)}$ and $P(x, y, t)$ can be approximately written as a product of $C(x, t)$ and $\rho(y; x)$, i.e., $P(x, y, t) \cong C(x, t)\rho(y; x)$. Taking into account the above relations, the dynamics of the system in the reduced dimension can be expressed as follows:

$$\frac{\partial C(x, t)}{\partial t} = \frac{\partial}{\partial x} D(x) \exp\left[-\frac{A(x)}{T(x)}\right] \frac{\partial}{\partial x} \exp\left[\frac{A(x)}{T(x)}\right] C(x, t) + \frac{\partial}{\partial x} [\mu(x) T'(x)] C(x, t). \quad (2.12)$$

In deriving the above equation, we note that the third term of the right hand side of Eq. (2.11) vanishes because $\int dy U(x, y) P(x, y, t) = 0$. One can obtain this result by integrating the function by parts and neglecting the irrelevant constant term. The terms of Eq. (2.12) can be readjusted to represent the equation in the following form:

$$\frac{\partial C(x, t)}{\partial t} = \frac{\partial}{\partial x} \mu(x) \left[A'(x) + T'(x) - A(x) \frac{T'(x)}{T(x)} \right] C(x, t) + \frac{\partial}{\partial x} D(x) \frac{\partial}{\partial x} C(x, t). \quad (2.13)$$

The modified Fick-Jacobs equation as derived above represents the reduced description of the dynamics for the system with irregular cross-sectional width and nonuniform temperature. This is the starting point of our analysis and can be considered as one of the central results of our study. The first term of the right hand side of Eq. (2.13) can be considered as the effective drift term and the second term takes care of the diffusion in the system having space dependent temperature. The interesting point to note here is that in the Langevin equation [Eq. (2.6)] the diffusion coefficient $D(x)$ guides the overall dynamics whereas in the Fokker-Planck description [Eqs. (2.9)–(2.13)], $\mu(x)$ and $T(x)$ make their presence independently. If we concentrate closely, it can be realized that the diffusion terms in the Fokker-Planck description depend on $D(x)$ which agrees well with the fact that the diffusion coefficient in the Langevin dynamics is connected to the fluctuating term. However, in the drift term temperature gradient appears. *The spatial variation of temperature actually modifies the effective potential of the system.* The two-dimensional Langevin dynamics [Eq. (2.8)] reduces to the two-dimensional Fokker-Planck equation [Eq. (2.9)] by considering very high value of $\gamma(x)$ [67] which ultimately reduces to the one-dimensional Fick-Jacobs equation [Eq. (2.13)] after consideration of local equilibrium description of Zwanzig along the transverse direction. The effective potential in this description can be extracted from the drift term as

$$V_{\text{eff}}(x, T(x)) = A(x) + T(x) - \int dx A(x) \frac{T'(x)}{T(x)} = A(x) + T(x) - A(x) \ln T(x) + \int dx A'(x) \ln T(x). \quad (2.14)$$

The explicit expression for $A(x)$ can be calculated using the previous relations. In the present case with a constant force acting along the negative y direction and the boundary functions given in Eq. (2.7), the potential function $A(x)$ reads as

$$A(x, T(x), G) = -T(x) \ln \left\{ \frac{2T(x)}{G} \sinh \left[\frac{G\omega(x)}{T(x)} \right] \right\}. \quad (2.15)$$

It is evident from the expression of Eq. (2.15) that the consideration of the presence of the weak force G like gravity along the negative y direction is crucial to realize the form of the effective potential in the reduced dimension. In the very high $G/T(x)$ limit, the Brownian particle explores the regions in the proximity of the lower boundary of the system recovering the effect of an energetic bistable potential. The limit $G/T(x) \rightarrow 0$ corresponds to the entropy-dominated situation, i.e., the overall effects appear due to the nontrivial influence of the boundary. G is a parameter which can be used to tune the system between the energy-dominated and entropy-dominated regimes [17]. In the entropy-dominated situation [i.e., in the limit $G/T(x) \rightarrow 0$]

which is at the focus of our current study, the expression of $A(x, T(x), G)$ reduces to

$$A(x, T(x)) = -T(x) \ln[2\omega(x)]. \tag{2.16}$$

Therefore, the expression for the effective potential $V_{\text{eff}} \ln(x, T(x) \ln)$ [Eq. (2.14)] clearly suggests that both the effects of the irregular cross-sectional width [appearing through the term $\omega(x)$ in $A(x)$] and nonuniform temperature [involving the terms $T(x)$] are well represented in the dynamical equation of the Brownian particles moving in a confined space. It is also evident from the above expression for V_{eff} that the potential of the system is an explicit function of the temperature of the system.

C. Blow-torch effect and the relative stability of the entropic states

The effective potential for the system where a particular area has been heated at a higher temperature [as shown in Fig. 1(b)] has been depicted in Fig. 2. We consider two heat baths which are isolated from each other but connected to the system [67]. The arrangement is such that the overall system is thermalized at a temperature T_0 and an additional high temperature bath with temperature T_1 is placed within the range x_l and x_r . That means whenever the Brownian particle comes within this interval, it interacts with the high temperature bath [3,67]. The span of the heated region is such that the particle can arrive at a local equilibrium with the high temperature bath [3] whereas the rest of the system is thermalized at temperature T_0 . For any coordinate x , at a particular temperature T , the effective potential $V_{\text{eff}}(x, T)$ takes the following form:

$$V_{\text{eff}}(x, T) = A(x) + T = -T \ln[2\omega(x)] + T. \tag{2.17}$$

The last two terms of Eq. (2.14) cancel each other because for a given zone $T(x)$ is constant. The plot of the effective potential in Fig. 2 follows from the above expression [Eq. (2.17)] using appropriate values of T_0 and T_1 for the low and the high temperature regions. Following van Kampen's prescription [67], we calculate the steady state relative population density of the two lobes. When the Brownian particle enters the hot region at x_l and leaves the region at x_r , it withdraws energy $V_{\text{eff}}(x_r) - V_{\text{eff}}(x_l)$ from the high temperature bath leading to the entropy change for that bath $-\frac{V_{\text{eff}}(x_r) - V_{\text{eff}}(x_l)}{T_1}$. The low temperature bath receives the equal amount of energy which gives rise to an increase in entropy, given by $\frac{V_{\text{eff}}(x_r) - V_{\text{eff}}(x_l)}{T_0}$. Therefore, $V_{\text{eff}}(x_r) - V_{\text{eff}}(x_l)$ amount of energy is transferred from the high temperature bath to the low temperature bath

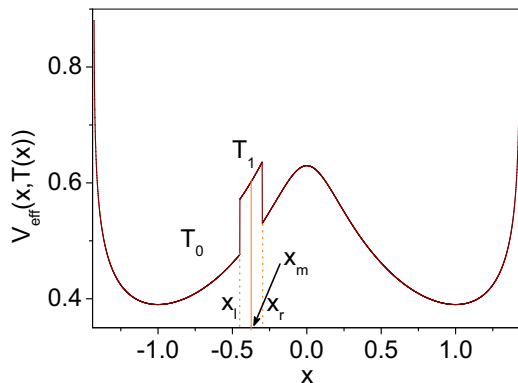


FIG. 2. (Color online) Effective potential of the system subjected to local heating. The system is in contact with the high temperature bath (temperature T_1) within the x range between x_l and x_r and with the low temperature bath (temperature T_0) elsewhere.

and the total entropy change for the system is given by $[V_{\text{eff}}(x_r) - V_{\text{eff}}(x_l)]\left[\frac{1}{T_0} - \frac{1}{T_1}\right]$. The probability of finding the particle at the right side of x_r increases in the steady state of the system subjected to spatially varying temperature compared to that of the system with a single temperature bath at temperature T_0 , by the exponential factor of the entropy increase for the process. The relative population density in the steady state in this situation can be expressed as follows:

$$\frac{P_{\text{right}}^{\text{st}}}{P_{\text{left}}^{\text{st}}} = \frac{P_{\text{right}}^{\text{eq}}}{P_{\text{left}}^{\text{eq}}} \exp\left\{ [V_{\text{eff}}(x_r) - V_{\text{eff}}(x_l)] \left(\frac{1}{T_0} - \frac{1}{T_1} \right) \right\}. \tag{2.18}$$

Here, $P_{\text{right}}^{\text{st}}$ and $P_{\text{right}}^{\text{eq}}$ refer to the integrated probability for the right lobe at the nonisothermal steady state and isothermal equilibrium state, respectively. $P_{\text{left}}^{\text{st}}$ and $P_{\text{left}}^{\text{eq}}$ denote the same for the left lobe. Using the explicit form of $V_{\text{eff}}(x, T)$ according to Eq. (2.17), we get

$$\frac{P_{\text{right}}^{\text{st}}}{P_{\text{left}}^{\text{st}}} = \frac{P_{\text{right}}^{\text{eq}}}{P_{\text{left}}^{\text{eq}}} \exp\left[-\left(\frac{T_1}{T_0} - 1 \right) \{ \ln[2\omega(x_r)] - \ln[2\omega(x_l)] \} \right]. \tag{2.19}$$

This is another key finding of this paper. The argument of the exponential is positive implying enhancement of relative population at the right lobe due to the heating at the left lobe. The amplification effect appears as a result of the local heating that alters the relative stability of the two entropic states which are characterized by the geometry or the wall function of the bilobal system. This may be considered as the Landauer's blow-torch effect in systems with entropic potential.

III. NUMERICAL SIMULATIONS IN TWO DIMENSIONS AND DISCUSSIONS

We now examine in detail the effect of zonewise heating of the bilobal enclosure to observe Landauer's blow-torch effect in physical confinement having nonuniform cross-sectional width which gives rise to an effective entropic potential in reduced dimension. The idea is to observe how local heating in one entropic state of the system gives rise to the population transfer to the other entropic state. These two states are separated by a barrier which bears both the characteristics of variation of cross section of the confinement, as well as of the nonuniformity of temperature along the structure. By entropic states, we refer to the left and the right lobes of the bilobal enclosure. For computational purpose, full numerical simulation of Eq. (2.6) in two dimensions along with the appropriate boundary conditions [Eq. (2.7)] is implemented. Thus, the motion of the Brownian particle remains essentially free as $G/D \rightarrow 0$; the only constraint imposed is that it cannot move out of the given boundary. There is no

conventional potential energy barrier present in the system. The dynamics of the particles is affected only by the influence of the boundary. Therefore, the effect of local heating which is manifested in the altered steady state population density of the two lobes considering a large ensemble of such system appears solely as the influence of varying boundary functions of the system.

It has been pointed out earlier [1] that the details of the noise processes of the entire path connecting the competing states are important to obtain the actual steady state population density in these states. This fact triggers our interest to understand how local heating of different zones of the same width of the left lobe alters the steady state population density in the right lobe. To this end, we quantitatively estimate two different descriptors. The first one is the reduced probability density as a function of x coordinate, i.e., $C(x,t) = \int_{\omega_l(x)}^{\omega_r(x)} P(x,y,t)dy$. The second one is the integrated probability of residence of the particles in one of the two lobes. The first quantity reflects how the probability distribution along the longitudinal direction gets modified due to spatial variation of temperature along that direction and the second one keeps a measure of the overall populations of the two entropic states which are being changed by the effect of zonal heating.

A. Reduced probability distribution

As mentioned above, the two-dimensional Langevin equation [Eq. (2.6)] is solved subjected to the boundary condition [Eq. (2.7)] using improved Euler algorithm with $\Delta t = 10^{-2}$. The white, Gaussian noise terms in Eq. (2.6) have been generated using the Box-Muller algorithm. The diffusion coefficient present in the noise term takes care of both the temperature as well as the damping constant of the system as depicted by the dimensionless description of the system. For different zones (the locally heated zone and the zones in thermal equilibrium with the low temperature bath), we use different and appropriate $D(x)$ which reflects the effect of varying temperature and viscosity of the medium. Say, the temperature, damping constant, and the diffusion coefficient of the original system are T_0 , γ_0 , and $D_0 = T_0/\gamma_0$ and those of the heated area are T_1 , γ_1 , and $D_1 = T_1/\gamma_1$, respectively. During the numerical solution of the Langevin dynamics [Eq. (2.6)], we take the value of $\gamma(x)$ and $T(x)$ at the beginning of the time step obeying the Itô interpretation [69]. It has been argued [70] that in systems with varying friction coefficient, both the Itô [69] and Stratonovich [71] descriptions may not lead to the correct equilibrium distribution in the overdamped limit. The ‘‘isothermal’’ (Hänggi) convention [72] which takes into account the damping coefficient at the end of the time step produces correct equilibrium distribution. However, during our numerical simulation study for the *exact two-dimensional system*, it has been observed that integrating the equations [Eq. (2.6)] obeying Itô’s convention gives physically consistent data irrespective of the position of the heated zone. The solutions obtained employing the ‘‘isothermal’’ description do not exhibit proper steady state behavior when the position near the bottleneck is heated. This may be due to the fact that the ‘‘isothermal’’ convention might not be applicable to systems having dimension higher than one to get correct equilibrium state distribution [73]. The second point is that in our case

the variation of $\gamma(x)$ or $T(x)$ is not continuous. The particle encounters the change of the environment not very frequently as the span of the low temperature region is considerably large and that of the heated area is sufficient to account for the local thermal equilibrium. Therefore, the consideration of the parameters at the beginning of the time step (Itô’s description) is supposed not to affect the correct portrayal of the steady state behavior of the system. Recent articles [70] describe novel methods for the simulation of Langevin dynamics in inhomogeneous media. However, as we are not dealing with inertial Brownian dynamics and concentrate on the particular choice of inhomogeneity as described here, we simulate the Langevin dynamics obeying Itô’s prescription. Throughout our numerical study, we have used the following values of the parameters: $a = 0.025$, $b = 0.05$, $c = 0.005$, and $G = 0.00001$. We consider symmetric structure of the enclosure. To study the reduced probability distribution for the system, we consider 6×10^6 number of trajectories. It has been checked carefully that the reduced probability density function indeed converges for the given number of trajectories. Initially, all the Brownian particles of the ensemble are kept at the middle of the bottleneck and allowed to evolve for sufficiently long time so that the ensemble attains a steady state distribution. This particular choice of initialization has been taken into account to ensure the equal occupancy of both the lobes immediately after the initial time step. It is convenient to compare the relative population transfer as a result of local heating with respect to a symmetric initial integrated probability density for the entropic states of comparable stability. This is actually equivalent to the random initialization which also gives rise to equal integrated probability density for each lobes initially. We are interested in the steady state properties of the system. Initial condition will have no effect on the steady state probability distribution or integrated probability of residence of the particles in either of the two lobes as the initial history is not retained due to the presence of noise in the system. In presence of a single heat bath, the particles are expected to accumulate around the positions of the maximal width of the structure in the left and the right lobes giving rise to two peaks of same height in the steady state probability distribution curve. When we consider local heating in a selected region of a lobe, say the left lobe, the total probability density of that lobe decreases and that of the other lobe (right lobe) increases eventually. The probability density naturally decreases at the domain which is kept at a higher temperature because the particles of the ensemble at this region gain higher kinetic energy from the bath and move faster from this area [3]. Therefore, the probability to find the particles in this region decreases, leading to a lower probability density of the particles in the heated zone. When the Brownian particles are in the heated lobe (here left lobe), they move faster towards the bottleneck. Consequently, the reduced probability density of the particles in the right lobe increases. One point regarding the existence of the local thermal equilibrium in the system should be addressed here. The Brownian particles do not carry inertia from the hot to the cold region. We have considered the overdamped limit of the dynamics of the Brownian particles and it does not allow for any inertia. Therefore, the temperature profile of the system remains unchanged. The overall effect of local heating is the altered population density in the steady state. The interesting point of

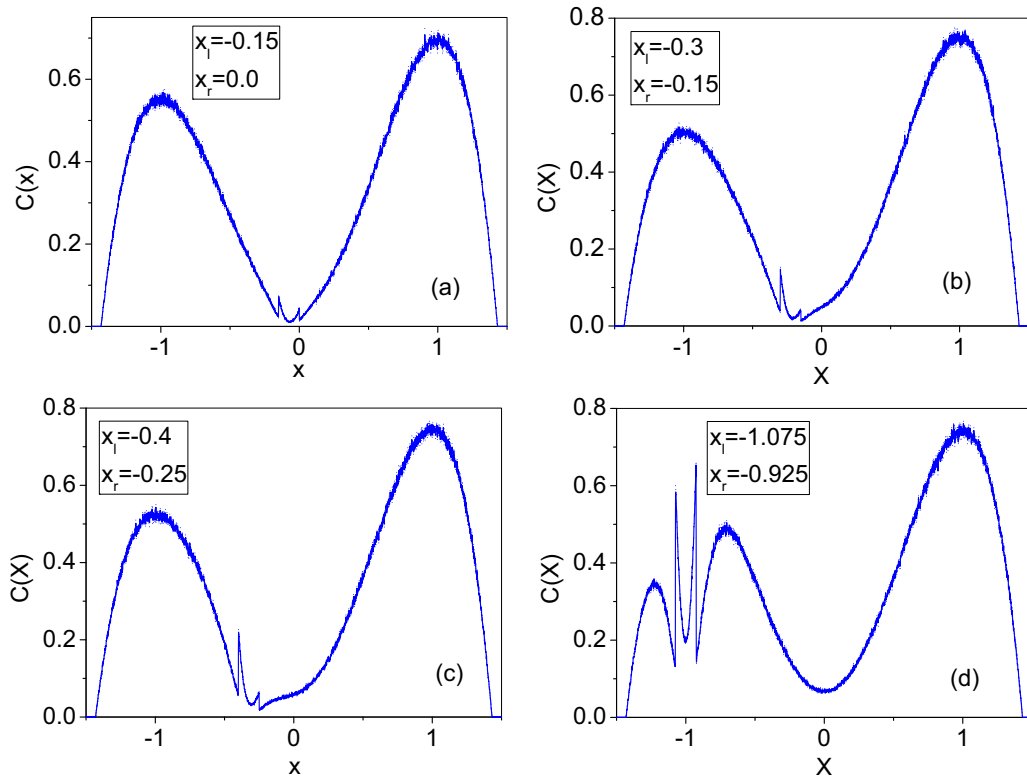


FIG. 3. (Color online) Probability distribution curve for the system with four different heated zones in the left lobe. The scaled diffusion coefficients of the low temperature and high temperature regions are $D_0 = 0.1$ and $D_1 = 2.0$, respectively.

observation is that not only the probability density centering the middle point of the heated zone decreases, but local humps are apparent at the proximity of the left and right boundaries of the hot area also. The appearance of local humps can be understood from the feature of the effective entropic potential which arises in the reduced description of the dynamics in the present setup. As there is an explicit temperature dependence of V_{eff} , the Brownian particles feel a different potential in the region which has been heated locally. It is evident from Eq. (2.17) and the plot of the potential having a heated zone (Fig. 2) that at the high temperature region, the potential experienced by the particles is higher compared to that for the isothermal case. This indicates that at the heated area, the velocity of the particles gets enhanced due to increased thermal fluctuation and the reformed potential energy curve implying the entropic nature of the effective potential. The feature is distinct since in the classical Landauer's blow-torch effect, only the velocity enhancement of the particles due to thermal effect [3] is encountered at the hot part of the system which reduces the probability to find the particles in that region giving rise to the altered probability distribution. The increased velocity of particles at the heated area causes depletion in the local probability density centering the midpoint of that zone, but no humps appear at the boundaries of the hot area. In the present system having varying cross-sectional width, the effective potential has two depressions at the left and the right boundaries of the high temperature domain due to the modification of the potential affected by local heating. As a consequence, the particle spends longer time than usual just before entering and after leaving the hot area at the

left and the right boundaries of the heated region, which it finds to have lower potential compared to its high temperature neighborhood. Away from the boundaries, the conventional dynamics takes over. The temperature dependence of the effective potential in the reduced description is reflected in the results obtained from full numerical simulations of the dynamics in two dimensions. The reduced probability distribution curves for the system with four different locally heated zones have been presented in Figs. 3(a)–3(d). All of these curves show depleted reduced probability density in the left lobe and rise of the same in the right lobe. Local humps are observed in all of these cases near the boundaries of the heated zone.

The difference in the diffusion coefficients (i.e., temperature) has been kept much higher in all the cases represented by Figs. 3(a)–3(d) to exhibit prominently the process of population transfer due to Landauer's blow-torch effect in the system characterized by varying cross section. When we are solving the actual dynamics of the system for numerical purpose, there is no problem at all to consider the above difference in diffusion coefficients. Moreover, in a real laboratory setup, two regions of such kind of system can be held at high temperature difference by using appropriate heat sources. For smaller temperature difference between the low and high temperature domains, the above-mentioned effects are observed in the probability distribution curve, but the height of the local humps in the distribution curve becomes smaller as expected. The probability distribution curves for smaller temperature difference have been shown in Figs. 4(a) and 4(b). The assumption of local equilibrium along the y

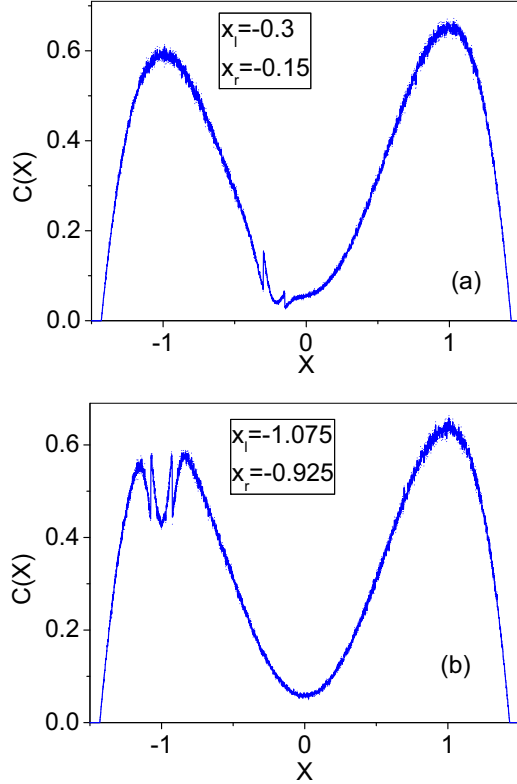


FIG. 4. (Color online) Probability distribution curve for the system with (a) $D_0 = 0.1$ and $D_1 = 0.6$ and (b) $D_0 = 0.1$ and $D_1 = 0.2$.

direction for reduced dynamical description also remains valid as the effective temperature dependent potential can explain the characteristics of the reduced probability distribution curve for the system obtained from full numerical simulations of the exact dynamics in two dimensions.

The results presented here are based upon the ensemble average of the observable quantities. We stress here that the system is ergodic. In order to verify this, we compare reduced probability density obtained by averaging over an ensemble of identical systems when they reach steady state and that obtained from a single trajectory considering the distribution of its longitudinal position variable starting from the initial condition and evolving up to a sufficiently long time. The comparison of the reduced probability density obtained from these two different considerations has been depicted in Fig. 5.

B. Dependence of population transfer on the detailed kinetics of the path connecting the entropic states

The extent of population transfer is measured in terms of the integrated probability of residence of the particles in the left and in the right lobes. We define the integrated probabilities as follows:

$$P_i(t) = \int_{\omega_l(x)}^{\omega_r(x)} dy \int_{x_0}^{\pm x_r} dx P(x, y, t), \quad (3.1)$$

where i stands for the left or the right lobe ($i = \text{left}, \text{right}$). x_0 is the x coordinate of the bottleneck position. To get the integrated probability in the left lobe, one has to integrate the distribution function over the entire y range starting from

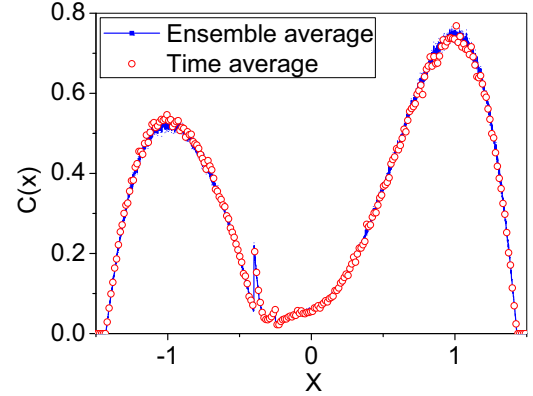


FIG. 5. (Color online) Checking ergodicity: reduced probability density curves calculated from the data of an ensemble of trajectories at the steady state and a single trajectory taking into account its longitudinal space variables during its evolution for the parameter set $D_0 = 0.1$ and $D_1 = 2.0$; $x_l = -0.4$ and $x_r = -0.25$.

x_0 to $-x_r$, the extreme left end of the structure. Similarly, for $P_{\text{right}}(t)$, the limit of the integration of the x range runs from x_0 to $+x_r$, the extreme right end of the enclosure. For the system kept at a constant temperature, both the lobes get equally occupied, at the steady state. This implies that the normalized integrated probability for both the lobes attains a value equal to 0.5 in the asymptotic limit. In case of the system with locally heated region in the left lobe as considered in this study, the values of $P_i(t)$ deviate from 0.5 in the steady state. The steady state value of $P_{\text{left}}(t)$, which is expressed as $P_{\text{left}}^{\text{st}}$, decreases from 0.5 and that for $P_{\text{right}}(t)$ (presented as $P_{\text{right}}^{\text{st}}$) rises above 0.5. This has been shown in Fig. 6. Here, $P_{\text{left}}(t)$ and $P_{\text{right}}(t)$ have been plotted against time for constant temperature throughout the system and for three different cases where the locally heated zone lies between

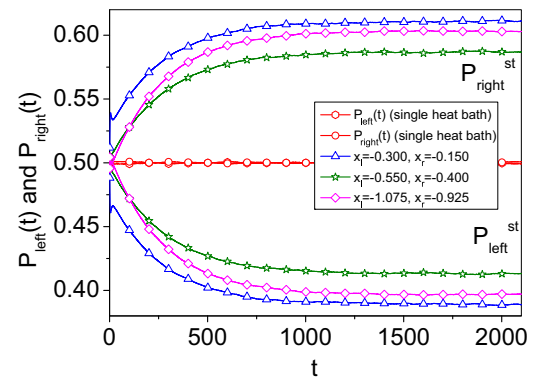


FIG. 6. (Color online) $P_{\text{left}}(t)$ and $P_{\text{right}}(t)$ plotted against time and attainment of the steady state value for the integrated probabilities. The lines with hexagonal and circular symbols correspond to the plot of $P_{\text{left}}(t)$ and $P_{\text{right}}(t)$ for the system with a single heat bath with diffusion coefficient $D_0 = 0.1$. The other three pairs of curves correspond to the case when the system is heated between three different x ranges of same width and for all these cases $D_0 = 0.1$ and $D_1 = 2.0$. The curves which saturate below 0.5 are the integrated probabilities for the left lobe and those saturate above 0.5 stand for the integrated probabilities for the right lobe.

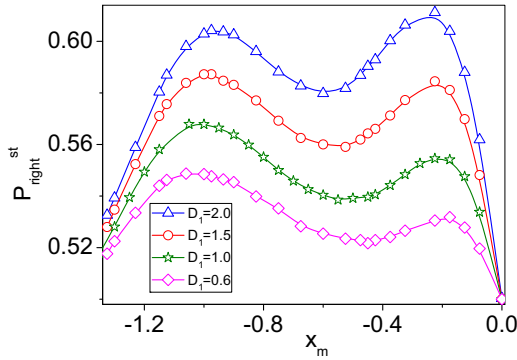


FIG. 7. (Color online) $P_{\text{right}}^{\text{st}}$ plotted against x_m for four different values of D_1 . D_0 has been kept fixed at 0.1 and the width $|x_l| - |x_r|$ has value equal to 0.15 for all four cases.

three different x ranges having the same width. The integrated probabilities have been calculated taking into consideration 10^6 trajectories. As expected, for the system with uniform temperature throughout its range, $P_{\text{left}}(t)$ and $P_{\text{right}}(t)$ saturate at 0.5. On the other hand, the steady state value of the integrated probabilities varies depending upon the position of the heated zone.

It is therefore apparent that the extent of population transfer will depend on the position of the region which has been kept at a higher temperature. We now examine the change in population density in terms of the integrated probability of residence of the particles in the right lobe. The higher value of $P_{\text{right}}^{\text{st}}$ implies more effective transfer of particles through the bottleneck from the left lobe as a consequence of local heating. The variation of the $P_{\text{right}}^{\text{st}}$ with respect to the mean position of the heated zone x_m (x_m is the mean value of x_l and x_r ; its modulus value refers to the distance of the midpoint of the hot domain from the bottleneck position along the x axis) has been represented in Fig. 7 for four different values of D_1 keeping D_0 fixed. The steady state integrated probability for the right lobe ($P_{\text{right}}^{\text{st}}$) has been averaged over 10^6 number of trajectories. The value of the $P_{\text{right}}(t)$ has been recorded for each x_m after allowing all the particles of the ensemble to evolve for quite a long time so that the integrated probability for the right lobe reaches its steady state value. The most striking aspect of the variation of $P_{\text{right}}^{\text{st}}$ against x_m is that there occur two maxima in the plot signifying that heating around two particular domains separately of a given lobe maximizes population transfer in the other lobe. One maximum appears slightly away from the bottleneck position and the other centering the position of the maximal width of the structure in the left lobe. Furthermore, the extent of population transfer depends on the temperature difference between the high temperature and the low temperature regions as expected. For higher temperature difference, the proportion of transfer is higher. This is also evident in Fig. 7.

To gain further insight, we have examined the variation of the mean first passage time (MFPT) against x_m (Fig. 8) for the identical situations above. To calculate the MFPT, we take into account a large ensemble of trajectories. Initially, all the particles are kept at the extreme left end of the structure and the time of escape for the particle from the left lobe is measured

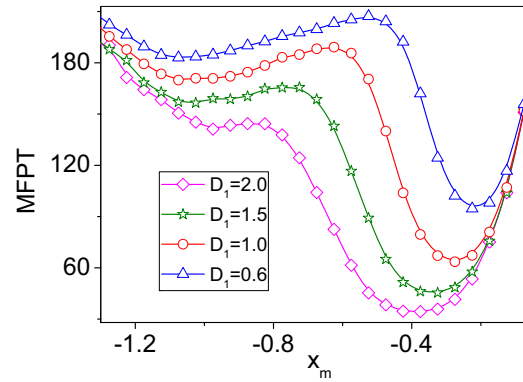


FIG. 8. (Color online) MFPT plotted against x_m for four different values of D_1 . D_0 has been kept fixed at 0.1 and the width $|x_l| - |x_r|$ has a value equal to 0.15 for all four cases.

and is averaged over the ensemble. This study is repeated for each x_m keeping the width of the heated zone fixed to get the intended variation. It is observed that the MFPT exhibits two minima when plotted against x_m . Similar to the previous case, one minimum corresponds to the position that lies between the bottleneck position and the position of the maximal width and the other one centers around the position of the maximal width of the structure. This fact supports that heating in the proximity of these two regions enhances the rate of escape from the left lobe leading to maximum integrated probability in the right lobe at the steady state.

The observed dependence of the effectiveness of the transfer of the particles on the position of the heated region follows exclusively from the influence of the confinement having varying width. The positions of the extrema near the bottleneck in both the $P_{\text{right}}^{\text{st}}$ versus x_m and MFPT versus x_m plot suggest that heating around these positions helps the particles to cross the bottleneck to maximum extent. This fact indicates that heating at the position of the bottleneck is less efficient to make the particles cross the entropic barrier compared to the heating at the region which lies slightly left to it. This finding is similar to that observed in case of the classical Landauer's blow-torch effect in presence of energetic barrier [8], which implies that supplying extra energy around this part of the system orients the particles mostly to cross the barrier by helping them to climb uphill in the effective entropic potential curve. Providing extra energy at the positions where orientation of the particles towards the constricted area can be done most efficiently enhances the efficacy of the transfer process, consequently increasing the proportion of transfer. The second maximum in the $P_{\text{right}}^{\text{st}}$ versus x_m plot which appears near the position of the maximal width of the structure bears pure signature of entropic transport. It has been pointed out by Zwanzig [11] that when a Brownian particle travels through physical confinement of varying width, the motion of the particle gets slowed down not only at the position of the bottleneck, but at the position of the bulge also. In the first case, the particle takes longer time to cross the bottleneck as it has to find its way through the narrow region, and for the latter case (near the bulge) it gets extra available space which it can explore through its random walk, thereby reducing the effectiveness of the directed transport. Therefore, the directed motion of the particle is affected at

the position of the maximal width of the structure. Energizing the particles in this region by using high temperature bath drives them away from this region. As the available phase space is more at the right side of the heated area, most of the particles move towards the bottleneck, thereby increasing the effectiveness of the entropic barrier crossing process. This effect manifests itself in the second minimum of the MFPT versus x_m plot and the second maximum of the $P_{\text{right}}^{\text{st}}$ when plotted against x_m . Heating around the position of the maximal width also affects maximum number of particles as the population is maximum at that position. Therefore, the steady state integrated probability density gets maximally altered due to heating at the above-mentioned region.

One pertinent point needs attention. The positions of the extrema of the plots for $P_{\text{right}}^{\text{st}}$ versus x_m and MFPT versus x_m are expected to overlap as the ratio $P_{\text{right}}^{\text{st}}/P_{\text{left}}^{\text{st}}$ is equal to the ratio of the transition rates over the barrier. However, the positions of the maxima in the $P_{\text{right}}^{\text{st}}$ versus x_m plot do not correspond exactly to the positions of the minima of the MFPT versus x_m plot. This deviation may arise due to the fact that to calculate the MFPT, we have kept all the particles initially at the extreme left end of the structure, i.e., we do not start with a Boltzmann distribution of particles within the left lobe. Therefore, the transition rate is not the inverse of the MFPT. Our considered initial condition brings another time scale into the system: the time scale of relaxation of the initial distribution to the Boltzmann distribution. Consequently, the positions of the extrema in the two above-mentioned plots do not overlap. The existence of two minima in the MFPT versus x_m plot corroborates qualitatively the appearance of the two maxima in the $P_{\text{right}}^{\text{st}}$ versus x_m plot.

Another fact needs clarification. As we are studying the entropic analog of Landauer's blow-torch effect, the heated areas of same width are considered to compare the steady state probabilities for differently heated regions.

To examine the variation of $P_{\text{right}}^{\text{st}}$ against x_m from the viewpoint of the effective reduced dynamics, we plot $P_{\text{right}}^{\text{st}}$ with respect to varying x_m obtained from the numerical solution of the one-dimensional Fick-Jacobs equation [Eq. (2.13)] or the corresponding Langevin equation. This dependence has been represented in Fig. 9. It is observed that the variation is qualitatively the same with that obtained from numerical findings.

IV. CONCLUSION

We have studied in detail the dependence of relative occupancy of two competing entropic states on the modified kinetics due to local heating in the path which connects these two states. The two lobes of a bilobal enclosure have been considered as the two entropic states. A portion of one of the lobes (here, the left lobe) is kept at a higher temperature to observe its effect on the relative stability or altered population density in the other lobe (right lobe). This may be considered as an entropic analog of Landauer's blow-torch effect. We summarize the main conclusions of this study as follows:

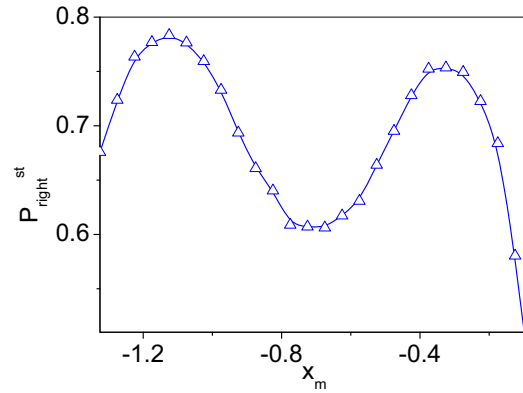


FIG. 9. (Color online) $P_{\text{right}}^{\text{st}}$ vs x_m plot obtained from the reduced description of the dynamics for $D_0 = 0.1$ and $D = 2.0$.

(i) On the basis of the reduced dynamical description of the process, we derive an effective entropic potential which bears, in addition to the characteristics of the varying cross section of the system, a clear signature of the nonuniform temperature along its length.

(ii) The blow-torch effect as well known in the energetic case leads to alteration of relative stability of the two entropic states.

(iii) The reduced probability distribution of the particles in the direction of transport calculated by full numerical simulation in two dimensions with appropriate boundary condition and considering a large ensemble of trajectories exhibits some characteristic features which can be explained by the nature of the effective entropic potential in reduced dimension.

(iv) The degree of population transfer in the right lobe at the steady state due to the heating at the left lobe depends in a very interesting way on the placement of the heated zone. A detailed two-dimensional Brownian dynamics simulation study reveals that there appear two maxima in the plot of the integrated probability of residence of the particles at the right lobe against the mean position of the high temperature region. These two maxima correspond to the positions of the heated area which maximize the effectiveness of the population transfer from one entropic state to the other implying that population transfer can be done most efficiently by heating around these two zones.

We conclude with a note that the current investigation is expected to have applicability in explaining phenomena related to population transfer processes occurring in real biological channels subjected to inhomogeneity of temperature and to model appropriate arrangements for entropic transport in geometry-controlled kinetics. We also believe that our findings may be useful to study the local heating effect on the kinetics of the chemical reactions which occur in a confined space having varying cross section.

ACKNOWLEDGMENTS

Thanks are due to the Council of Scientific and Industrial Research, Government of India, for partial financial support.

- [1] R. Landauer, *Phys. Scr.* **35**, 88 (1987).
- [2] R. Landauer, *J. Stat. Phys.* **53**, 233 (1988).
- [3] R. Landauer, *Phys. Lett. A* **68**, 15 (1978).
- [4] R. Landauer, *Phys. Rev. A* **15**, 2117 (1977).
- [5] R. Landauer, *J. Stat. Phys.* **13**, 1 (1975).
- [6] R. Landauer, *Phys. A (Amsterdam)* **194**, 551 (1993).
- [7] N. G. van Kampen, *Superlattices Microstruct.* **23**, 559 (1998).
- [8] M. Bekele, S. Rajesh, G. Ananthakrishna, and N. Kumar, *Phys. Rev. E* **59**, 143 (1999).
- [9] M. H. Jacobs, *Diffusion Processes* (Springer, New York, 1967).
- [10] H. Zhou and R. Zwanzig, *J. Chem. Phys.* **94**, 6147 (1991); R. Zwanzig, *Phys. A (Amsterdam)* **117**, 277 (1983).
- [11] R. Zwanzig, *J. Phys. Chem.* **96**, 3926 (1992).
- [12] D. Reguera and J. M. Rubi, *Phys. Rev. E* **64**, 061106 (2001).
- [13] D. Reguera, G. Schmid, P. S. Burada, J. M. Rubi, P. Reimann, and P. Hänggi, *Phys. Rev. Lett.* **96**, 130603 (2006); P. S. Burada, G. Schmid, D. Reguera, J. M. Rubi, and P. Hänggi, *Phys. Rev. E* **75**, 051111 (2007); S. Martens, G. Schmid, L. Schimansky-Geier, and P. Hänggi, *ibid.* **83**, 051135 (2011).
- [14] D. Mondal and D. S. Ray, *Phys. Rev. E* **82**, 032103 (2010).
- [15] P. S. Burada, G. Schmid, P. Talkner, P. Hänggi, D. Reguera, and J. M. Rubi, *BioSystems* **93**, 16 (2008).
- [16] D. Mondal, M. Das, and D. S. Ray, *J. Chem. Phys.* **133**, 204102 (2010).
- [17] P. S. Burada, G. Schmid, D. Reguera, M. H. Vainstein, J. M. Rubi, and P. Hänggi, *Phys. Rev. Lett.* **101**, 130602 (2008); P. S. Burada, G. Schmid, D. Reguera, J. M. Rubi, and P. Hänggi, *Eur. Phys. J. B* **69**, 11 (2009).
- [18] H. Ding, H. Jiang, and Z. Hou, *J. Chem. Phys.* **142**, 194109 (2015).
- [19] D. Mondal, M. Das, and D. S. Ray, *J. Chem. Phys.* **132**, 224102 (2010).
- [20] B. Q. Ai and L. G. Liu, *J. Chem. Phys.* **126**, 204706 (2007); *Phys. Rev. E* **74**, 051114 (2006).
- [21] D. Mondal, *Phys. Rev. E* **84**, 011149 (2011).
- [22] F. Marchesoni and S. Savelev, *Phys. Rev. E* **80**, 011120 (2009).
- [23] M. Das, D. Mondal, and D. S. Ray, *J. Chem. Sci.* **124**, 21 (2012).
- [24] D. Mondal and D. S. Ray, *J. Chem. Phys.* **135**, 194111 (2011); D. Mondal, M. Sajjan, and D. S. Ray, *J. Indian. Chem. Soc.* **88**, 1791 (2011).
- [25] B. Q. Ai and L. G. Liu, *J. Chem. Phys.* **128**, 024706 (2008); B. Q. Ai, H. Z. Xie, and L. G. Liu, *Phys. Rev. E* **75**, 061126 (2007); B. Q. Ai, Y. F. He, and W. R. Zhong, *J. Chem. Phys.* **141**, 194111 (2014).
- [26] B. Q. Ai, *J. Chem. Phys.* **131**, 054111 (2009); F. G. Li and B. Q. Ai, *Chem. Phys.* **388**, 43 (2011).
- [27] P. Margaretti, I. Pagonabarraga, and J. M. Rubi, *J. Chem. Phys.* **138**, 194906 (2013).
- [28] M. Borromeo, F. Marchesoni, and P. K. Ghosh, *J. Chem. Phys.* **134**, 051101 (2011).
- [29] F. Marchesoni, *J. Chem. Phys.* **132**, 166101 (2010).
- [30] A. M. Berezhkovskii, M. A. Pustovoit, and S. M. Bezrukov, *Phys. Rev. E* **80**, 020904(R) (2009); A. M. Berezhkovskii and S. M. Bezrukov, *Biophys. J.* **88**, L17 (2005).
- [31] I. D. Kosińska, I. Goychuk, M. Kostur, G. Schmid, and P. Hänggi, *Phys. Rev. E* **77**, 031131 (2008).
- [32] M. Muthukumar, *J. Chem. Phys.* **118**, 5174 (2003); *Phys. Rev. Lett.* **86**, 3188 (2001); J. K. Wolterink, G. T. Barkema, and D. Panja, *ibid.* **96**, 208301 (2006).
- [33] W. Sung and P. J. Park, *Phys. Rev. Lett.* **77**, 783 (1996); P. J. Park and W. Sung, *ibid.* **80**, 5687 (1998); K. Luo, T. Ala-Nissila, S.-C. Ying, and A. Bhattacharya, *ibid.* **99**, 148102 (2007); **100**, 058101 (2008).
- [34] J. A. Cohen, A. Chaudhuri, and R. Golestanian, *Phys. Rev. Lett.* **107**, 238102 (2011).
- [35] S. Van Dorp, U. F. Keyser, N. H. Dekker, C. Dekker, and S. G. Lemay, *Nat. Phys.* **5**, 347 (2009); Z. Siwy and A. Fulinski, *Phys. Rev. Lett.* **89**, 198103 (2002); Z. Siwy, I. D. Kosinska, A. Fulinski, and C. R. Martin, *ibid.* **94**, 048102 (2005).
- [36] P. Kalinay and J. K. Percus, *Phys. Rev. E* **72**, 061203 (2005); **74**, 041203 (2006); *J. Stat. Phys.* **123**, 1059 (2006); *Phys. Rev. E* **78**, 021103 (2008).
- [37] P. Kalinay, *Phys. Rev. E* **80**, 031106 (2009); **84**, 011118 (2011); **87**, 032143 (2013); **89**, 042123 (2014).
- [38] P. Kalinay and J. K. Percus, *Phys. Rev. E* **83**, 031109 (2011).
- [39] P. Kalinay and J. K. Percus, *J. Chem. Phys.* **129**, 154117 (2008).
- [40] D. Reguera, A. Luque, P. S. Burada, G. Schmid, J. M. Rubi, and P. Hänggi, *Phys. Rev. Lett.* **108**, 020604 (2012); T. Motz, G. Schmid, P. Hänggi, D. Reguera, and J. M. Rubi, *J. Chem. Phys.* **141**, 074104 (2014).
- [41] R. M. Bradley, *Phys. Rev. E* **80**, 061142 (2009).
- [42] P. S. Burada and G. Schmid, *Phys. Rev. E* **82**, 051128 (2010).
- [43] C. Valero Valdes and R. Herrera Guzman, *Phys. Rev. E* **90**, 052141 (2014).
- [44] G. Forte, F. Cecconi, and A. Vulpiani, *Phys. Rev. E* **90**, 062110 (2014).
- [45] G. P. Suárez, M. Hoyuelos, and H. O. Martín, *Phys. Rev. E* **91**, 012135 (2015).
- [46] A. M. Berezhkovskii, M. A. Pustovoit, and S. M. Bezrukov, *J. Chem. Phys.* **126**, 134706 (2007).
- [47] L. Dagdug, A. M. Berezhkovskii, Y. A. Makhnovskii, V. Y. Zitserman, and S. M. Bezrukov, *J. Chem. Phys.* **136**, 214110 (2012).
- [48] L. Dagdug, M. V. Vazquez, A. M. Berezhkovskii, and S. M. Bezrukov, *J. Chem. Phys.* **133**, 034707 (2010); L. Dagdug, M. V. Vazquez, A. M. Berezhkovskii, V. Y. Zitserman, and S. M. Bezrukov, *ibid.* **136**, 204106 (2012); L. Dagdug and I. Pineda, *ibid.* **137**, 024107 (2012); I. Pineda, J. Alvarez-Ramirez, and L. Dagdug, *ibid.* **137**, 174103 (2012).
- [49] G. Chacón-Acosta, I. Pineda, and L. Dagdug, *J. Chem. Phys.* **139**, 214115 (2013); A. A. García-Chung, G. Chacón-Acosta, and L. Dagdug, *ibid.* **142**, 064105 (2015).
- [50] K. D. Dorfman and E. Yariv, *J. Chem. Phys.* **141**, 044118 (2014).
- [51] B. Q. Ai, Z. G. Shao, and W. R. Zhong, *J. Chem. Phys.* **137**, 174101 (2012); B. Q. Ai, Q. Y. Chen, Y. F. He, F. G. Li, and W. R. Zhong, *Phys. Rev. E* **88**, 062129 (2013).
- [52] B. Q. Ai, Y. F. He, F. G. Li, and W. R. Zhong, *J. Chem. Phys.* **138**, 154107 (2013); X. T. Zheng, J. C. Wu, B. Q. Ai, and F. G. Li, *Eur. Phys. J. B* **86**, 479 (2013).
- [53] B. Q. Ai and J. C. Wu, *J. Chem. Phys.* **139**, 034114 (2013).
- [54] X. G. Huang, P. Deng, and B. Q. Ai, *Phys. A (Amsterdam)* **392**, 411 (2013); Y. Liu and B. Q. Ai, *J. Phys.: Condens. Matter* **21**, 465102 (2009); F. G. Li and B. Q. Ai, *J. Stat. Mech.* (2014) P04027; *Phys. Rev. E* **87**, 062128 (2013).
- [55] J. C. Wu, Q. Chen, R. Wang, and B. Q. Ai, *Chaos* **25**, 023114 (2015).
- [56] Q. Chen, B. Q. Ai, and J. W. Xiong, *Chaos* **24**, 033119 (2014).
- [57] K. K. Mon, *J. Chem. Phys.* **129**, 124711 (2008).

- [58] O. Benichou, C. Chevalier, J. Klafter, B. Meyer, and R. Voituriez, *Nat. Chem.* **2**, 472 (2010).
- [59] O. Benichou and R. Voituriez, *Phys. Rev. Lett.* **100**, 168105 (2008).
- [60] M. Borromeo and F. Marchesoni, *Chem. Phys.* **375**, 536 (2010).
- [61] D. Mondal, M. Das, and D. S. Ray, *Phys. Rev. E* **85**, 031128 (2012).
- [62] M. Das, D. Mondal, and D. S. Ray, *J. Chem. Phys.* **136**, 114104 (2012).
- [63] M. Das, D. Mondal, and D. S. Ray, *Phys. Rev. E* **86**, 041112 (2012); M. Das and D. S. Ray, *ibid.* **88**, 032122 (2013).
- [64] M. Das, *Phys. Rev. E* **89**, 032130 (2014); **90**, 062120 (2014).
- [65] J. Werner and M. Buse, *J. Appl. Physiol.* **65**, 1110 (1988).
- [66] H. Risken, *The Fokker-Planck Equation*, 2nd ed. (Springer, Berlin, 1989).
- [67] N. G. van Kampen, *IBM J. Res. Dev.* **32**, 107 (1988).
- [68] N. G. van Kampen, *J. Math. Phys.* **29**, 1220 (1988).
- [69] K. Itô, *Proc. Imp. Acad. Tokyo* **20**, 519 (1944).
- [70] O. Farago and N. Gronbech-Jensen, *Phys. Rev. E* **89**, 013301 (2014); *J. Stat. Phys.* **156**, 1093 (2014).
- [71] R. L. Stratonovich, *SIAM J. Control* **4**, 362 (1966).
- [72] P. Hänggi, *Helv. Phys. Acta* **51**, 183 (1978).
- [73] M. Hütter and H. C. Öttinger, *J. Chem. Soc., Faraday Trans.* **94**, 1403 (1998).